Source complexity effects on ground shaking scenarios

D. SANDRON, P. SUHADOLC and G. COSTA

Department of Earth Sciences, University of Trieste, Italy

ABSTRACT　　Hazard analysis requires the parameterization of the seismic sources that can be expected to affect a selected place in terms of locations, magnitudes, focal mechanism and, for event with a significant magnitude, the dimension of the fault and the distribution of the slip on the fault surface. We use a kinematic approach to compute ground shaking scenarios, through the modelling of the source geometry and of the seismic moment distribution on the fault surface. We investigate three events: the M_w 5.2 Bovec (Slovenia) July 2004 one and the two M_w 6.5 Iceland June 2000 ones. We present the results in terms of contour map of the maximum horizontal ground acceleration extracted from the synthetics calculated on a grid of receivers equally spaced around the fault area. To reproduce the surface fault complexity we considered: a) a uniform seismic moment distribution; b) a seismic moment distribution with a single asperity located in the central part of the fault surface; c) a seismic moment distribution with two asperities and d) in one case the seismic moment distribution obtained from the inversion of strong ground motion data. Our results confirm that the slip distribution, and in particular the position of the asperities on the fault plane, plays a non-negligible role in seismic hazard assessment. If, in the future a variety of more or less characteristic slip distributions for a given set of faults in an active tectonic area can be assessed, the possible source-related variability of expected ground motion shaking in the region could be easily estimated.

1. Overview

The study of strong ground motion, earthquake hazard and risk plays an important role in seismology and in the sustainable development of economies and societies. The principal goals of strong motion seismology are to improve the scientific understanding of the physical processes that control strong ground shaking and to develop reliable estimates of seismic hazard, for the reduction of loss of life and property during future earthquakes. Hazard analysis requires the parameterization of the seismic sources that can be expected to affect a selected place in terms of locations, magnitudes, focal mechanism and, for event with a significant magnitude, the dimension of the fault and the distribution of the slip on the fault surface. Knowledge of the attenuation of ground motion with the epicentral distance, integrated whenever possible with realistic modeling of seismic wave propagation, and knowledge of the local geology for site-specific assessments, will promote this analysis to a large extent. The output of seismic hazard analysis can be a description of the intensity of shaking at a site due to a nearby earthquake of a certain magnitude or a map which shows levels of ground shaking in various parts of the country that have an equal probability of being exceeded. If a deterministic approach is used to

characterize the ground motion, then a single scenario earthquake is usually used to represent the seismic hazard at a given site (the event producing the maximum acceleration at the site), and its frequency of occurrence does not directly influence the level of the hazard. Scenarios for different magnitude earthquakes associated with active faults in the Alps-Dinaridies region have been evaluated by Fiztko *et al*. (2004). Detailed studies of the spatial distribution of slip on the fault plane for earthquakes in tectonically active regions, show that the slip distribution is rather variable, characterized by regions of large slip surrounded by regions of low slip. The slip distribution on the fault, in particular the position of the asperities, plays a non-negligible role on the shape and position of zones in the surroundings of the earthquake that are subject to high ground shaking (e.g. Somerville and Moriwaki, 2003). In this paper, we show how the slip distribution on the fault affects the ground shaking in its surroundings by applying our procedure to three events in Slovenia and Iceland.

2. Computational outline

In our strong ground motion scenarios, we model the extended source using a kinematic approach. In the computation of the synthetic seismograms we assume an a priori seismic moment distribution, which is a function of time and space. In this way, we do not relate it to the stress that caused it.

The fracture process is described purely by the slip vector as a function of the coordinates on the fault plane, and of the rupturing time. The synthetic seismograms are computed using the method of the Modal Summation (Panza, 1985; Panza and Suhadolc, 1987; Florsch *et al*., 1991; Panza *et al*., 2001) for extended sources (Saraò *et al*., 1998). The maximum frequency content in the synthetics is 1 Hz, as a consequence of the degree of knowledge of the available structural model. To go higher than a few Hz one should use a hybrid approach (e.g. Kamae *et al*., 1998), i.e. a combination of a kinematic model (like ours) at low frequencies (< 1 Hz) and a stochastic method at high frequencies (>1 Hz). In our approach, the synthetic seismograms are computed assuming that all the sites lie on bedrock. The rupture surface is approximated as a planar surface defined by a length L and a down dip extent W, whose dimensions vary according to the scalar seismic moment M_0 of the event (Wells and Coppersmith, 1994). The time dependency of the seismic moment release is described using a rupture propagation model that requires to fix the position of the nucleation point on the fault, and the rupture propagation velocity, which is assumed to be constant (usually around 70% of the shear waves velocity). The source parameters of strike, dip and rake are chosen according to the known geometry of active faults and/or historical earthquakes in the area.

In the computations of the ground shaking scenarios we consider both a uniform and a non-uniform seismic moment distribution on the fault plane. In the simplest approach, we apply a constant seismic moment, and we smooth it at the fault edges by means of a cosine tapering function, in order to avoid possible border effects and to be compatible with the physics of fault rupturing. More reasonably, one should consider that the largest amount of seismic moment is usually concentrated in small areas on the fault plane, asperities, where the slip vector, proportional to M_0, is statistically 1.5 times or more larger than its average value (Sommerville *et al*., 1997). Moreover, there is no evident correlation between the hypocenter position and the
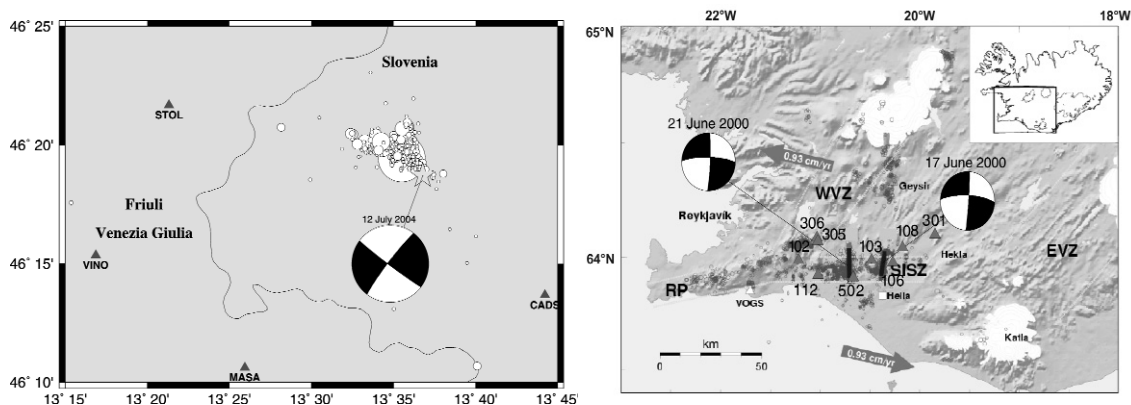
Fig. 1 - On the left: map zoom of the region around the 12 July 2004 Bovec event: the star shows the epicentre. The white circles represent the aftershocks scaled with magnitude. On the right: the south-western part of Iceland. Dotted lines denote the western volcanic zone (WVZ) and the eastern volcanic zone (EVZ). The South Iceland Seismic Zone (SISZ) is indicated as well as its prolongation in the Reykjanes peninsula (RP). The direction of the relative plate motion is shown by arrows. The faults of the two large earthquakes that ruptured on June 17 and 21 are indicated by 17 and 21, respectively, together with the aftershock distribution (dots). The grey numbered triangles are the stations of the Icelandic Strong-Motion Network used in the inversion (Sandron *et al.*, 2007).

maximum seismic moment release areas or the position of asperities. In a more realistic approach, we use the k^2 model (Herrero and Bernard, 1994) to construct seismic moment distributions on the fault surface, characterized either by a single asperity or by two asperities. A cosine tapering function is applied, also in this case, at the fault edges in order to avoid that the asperities be physically unrealistic. The ideal approach would be to use the real seismic moment distribution on the fault surface.

To solve the inverse problem for the source of a particular earthquake, that is to determine the spatial and temporal distribution of slip or slip rate over the fault area, we use the method of linear programming (Press *et al.*, 1986), following the formulation developed and applied to the earthquake faulting problem by Das and Kostrov (1990, 1994) and adapted to inversion of local recordings by Das and Suhadolc (1996). The best resulting seismic moment distribution can be used as input for the ground motion scenario.

We present our results as a contour map of the maximum horizontal ground acceleration extracted from the synthetics calculated on a grid of receivers equally spaced around the fault. The parameter used for gridding the data is equal to the distance between the receivers, and the tension factor is chosen according to the single cases. In this way, the contour maps reproduce the punctual results, without introducing distortions, and permit us to visualize also source directivity effects on the horizontal acceleration field.

3. Input seismic moment distribution on the fault surface: two simple examples

In the first earthquake scenario we model the strong ground motion affecting the Friuli Venezia Giulia region (NE Italy) caused by the 12 July 2004 M_w=5.2 Bovec (Slovenia) event. The
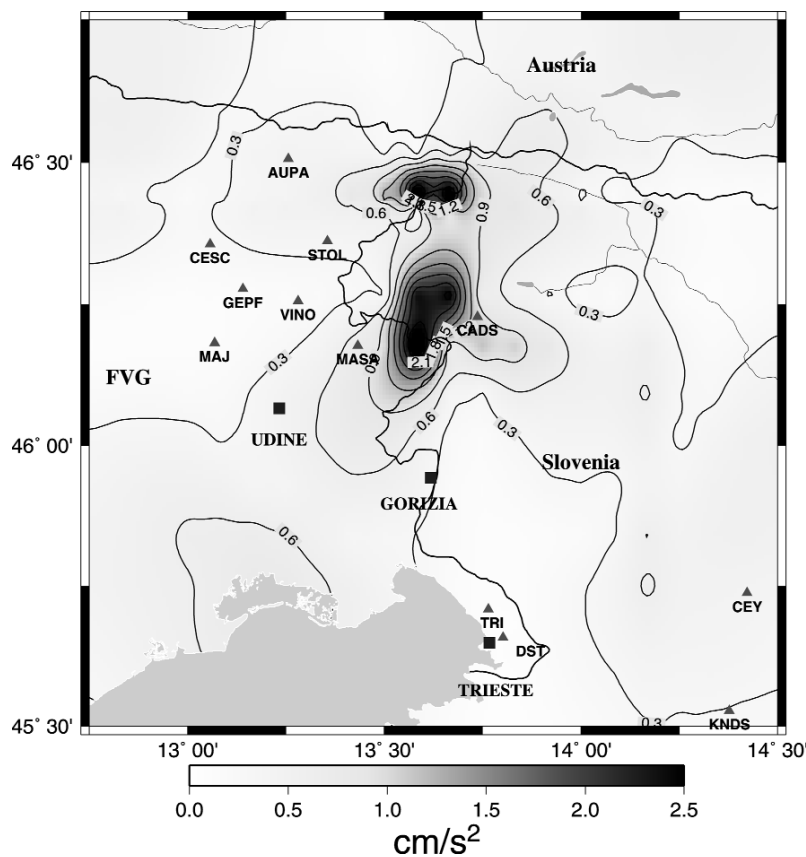
Fig. 2 - Contour maps of the resulting maximum horizontal spectral accelerations (the maximum frequency content is 1 Hz) calculated for an uniform seismic moment distribution corresponding to $M_0 = 3.5 \times 10^{18}$ $N \times m$ with a rupture that propagates bilaterally from the center of the fault.

area of study is located at the junction between the south-eastern Alps and the external Dinarides, a region covering north-eastern Italy and western Slovenia, respectively (Fig. 1). The seismic activity of this area is associated with a rather complex active deformation pattern: the Alpine compressive system is active on structures trending mainly E-W, while the Dinaric system, represented by segmented strike-slip faults, trends mostly NW-SE (Carulli *et al*., 1990; Aoudia, 1998; Fiztko, 2003). The input fault model parameters used in the synthetic seismogram computations are (Swiss Seismological Service, 2006): strike = 127°, dip = 87°, rake = 175°. As regards the geometry of the fault, we set its dimensions as follows: 5 km length, 4 km wide down-dip and with the top edge fixed at a 5 km depth. To reproduce the surface fault complexity we consider: a) a uniform seismic moment distribution corresponding to $M_0 = 3.5 \times 10^{18}$ $N \times m$ with a rupture that propagates bilaterally from the center of the fault; b) a seismic moment distribution with a single asperity located in the central part of the fault surface; and c) a seismic moment distribution with two asperities (even if rather unlikely for such a small fault): the bigger one placed near the western edge of the fault and the smaller one shifted toward E (Herrero and Bernard, 1994).

The map in Fig. 2 shows the maximum horizontal ground accelerations calculated in the simplest case of a uniform seismic moment distribution and in correspondence to 625 receivers, grid
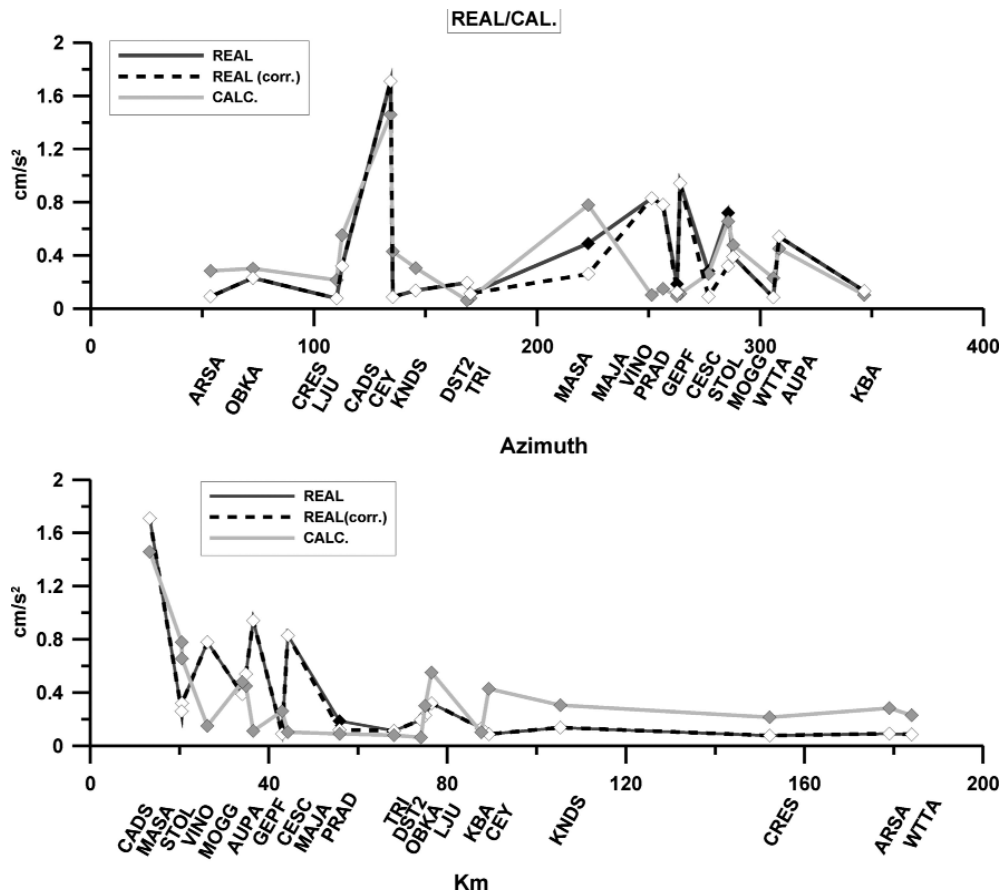
Fig. 3 - Comparison between the values of the maximum horizontal accelerations computed and the values, filtered at 1 Hz, recorded at the stations of the integrated network created among seismological institutions of Italy, Austria and Slovenia in the framework of an Interreg Project (see text).

arranged, and placed at a grid distance of 5 minutes in latitude and longitude over a territory that includes the Friuli Venezia Giulia (FVG afterwards) region, part of Slovenia and Austria. We compare our results with the real accelerations, filtered at 1 Hz, recorded at the stations belonging to the integrated network created in the seismic-prone Alpe-Adria region with the contribution of: Zentralanstalt für Meteorologie und Geodynamik, Hauptabteilung Geophysik, Wien, Österreich (ZAMG-AUT), Agencija Republike Slovenije za okolje, Urad za seizmologijo in geologijo, Ljubljana, Slovenija, (ARSO-SLO), Dipartimento di Scienze della Terra, Università degli Studi di Trieste, Trieste, Italia (DST-ITA), Istituto Nazionale di Oceanografia e di Geofisica Sperimentale – OGS, Italia (OGS-ITA) (http://www.dst.units.it/RAF06). We can analyze the trend of the values with the epicentral distance and azimuth. In spite of the simple approach, the overall agreement validates our approach (Fig. 3). At some stations the observed values are larger than the calculated ones, in particular for distances within 50 km. However, in the computation of the synthetic seismograms, we use a structural model that does not take into account the presence of the alluvional deposits near the surface which, as is well known, generally cause an
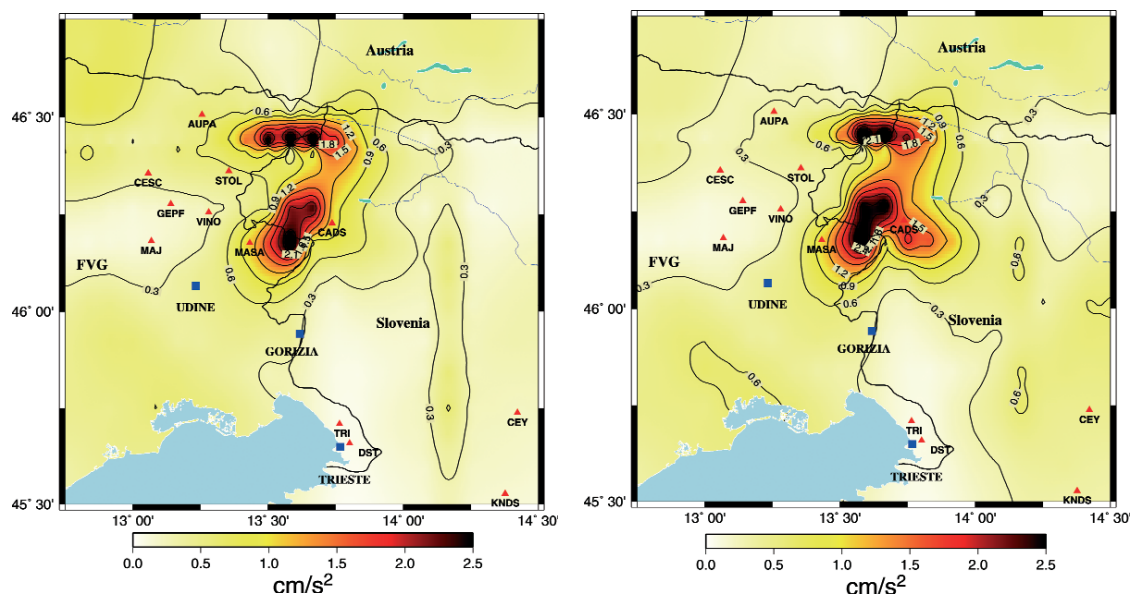
Fig. 4 - Contour maps of the resulting maximum horizontal spectral accelerations (the maximum frequency content is 1 Hz) calculated (on the left) from a seismic moment distribution with a single asperity corresponding to $M_0 = 3.5 \times 10^{18}$ $N \times m$ with a rupture that propagates bilaterally from the center of the fault; (on the right) the same but from a seismic moment distribution with two asperities.

amplification of the ground shaking (site effect). On the other hand, we have taken into account (Fig. 3, dashed line) the amplification factors estimated at some of the stations managed by DST-ITA (Costa *et al.*, 2006a). Since the site effect corrections are about a factor of two, the overall picture does not change much.

As a first example of how the complexity of the fault affects the shape and position of the high-acceleration zone around it, we calculate three scenarios using the three seismic moment distributions mentioned above for the Bovec event [case a), b) and c) in the following considerations]. Our results for case a) show (Fig. 2) that the maximum values of acceleration are located in Slovenia but they affect also the FVG region in its northernmost part, near the border with Austria, and in the zone NE of Udine. In case b) we can notice (Fig. 4 left) a prolongation of the region with greater accelerations towards west, particularly in the north of the FVG region near the station of AUPA. Low values of ground motion are expected in the inner part of Slovenia. In case c) we can note, instead, an enlargement of the maximum acceleration area towards SE, in correspondence to the station CADS, very near the epicentre (Fig. 4 right).

In general, applying a non-uniform seismic moment distribution, we compute accelerations that are larger than those produced using a uniform moment distribution. However, the accelerations decrease more rapidly with the distance between the fault and the site, since large portions of the fault radiate small values of seismic moment. This fact is even more evident in the case of a single asperity. For the case of a two-asperity seismic moment distribution, the ratio between the maximum seismic moments released at each asperity plays also an important role. Moreover, in our simple approach we fix the rupture to propagate bilaterally from the center of the fault. We
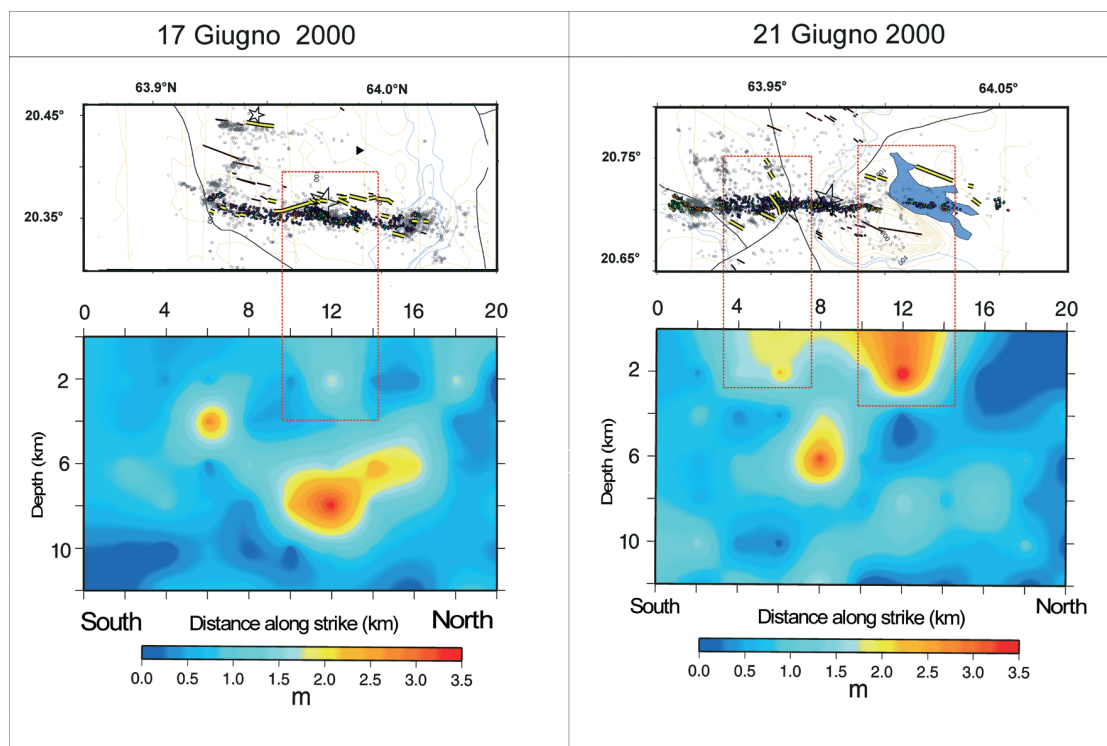
Fig. 5 - Map views (top) of the two June 2000 earthquakes aftershock distributions. The hypocenter of the main event is shown as a star. Our best slip distribution (bottom) obtained from the inversion of strong motion data (Sandron *et al*., 2007) is shown as a contour map. The dotted red boxcar points out the relationship between the observed surface fractures, displayed as yellow lines, and the surface slip.

do not consider, in this work, the further question concerning the position of the nucleation point and, as a consequence, of the direction of propagation, that could lead to the well-known directivity effect (Archuleta and Hartzell, 1981; Somerville *et al*., 1997).

The second scenario analyzes the ground shaking in the South Iceland Seismic Zone (SISZ) produced by the 17 and 21 June 2000 M_w=6.5 events. The two earthquakes occurred on parallel, N-S striking, right-lateral strike-slip faults, separated by about 17 km. The fault mechanism and the fault area are deduced from teleseismic centroid moment solutions and from aftershock distributions, respectively (Stefansson *et al*., 2003). The faults are taken as 20 km long and near-vertical, extending from the surface to a depth of approximately 15 km, for both earthquakes (Wells and Coppersmith, 1994). The synthetics are calculated over a 5km x 5km grid of receivers equally spaced around the fault region and we consider, in the simplest approach, a uniform seismic moment distribution on the fault plane, then we apply the "best" seismic moment distribution obtained from the inversion of strong motion data (Fig. 5) (Sandron *et al*., 2007). If we consider as input a uniform seismic moment distribution, corresponding to M_W =6.5 for both the events the resulting maximum values of spectral horizontal accelerations are almost at the same level (Fig. 6, top). Expected differences in the radiation pattern are due to different fault parameters among which, above all, the different nucleation cells. When we consider as input the seismic
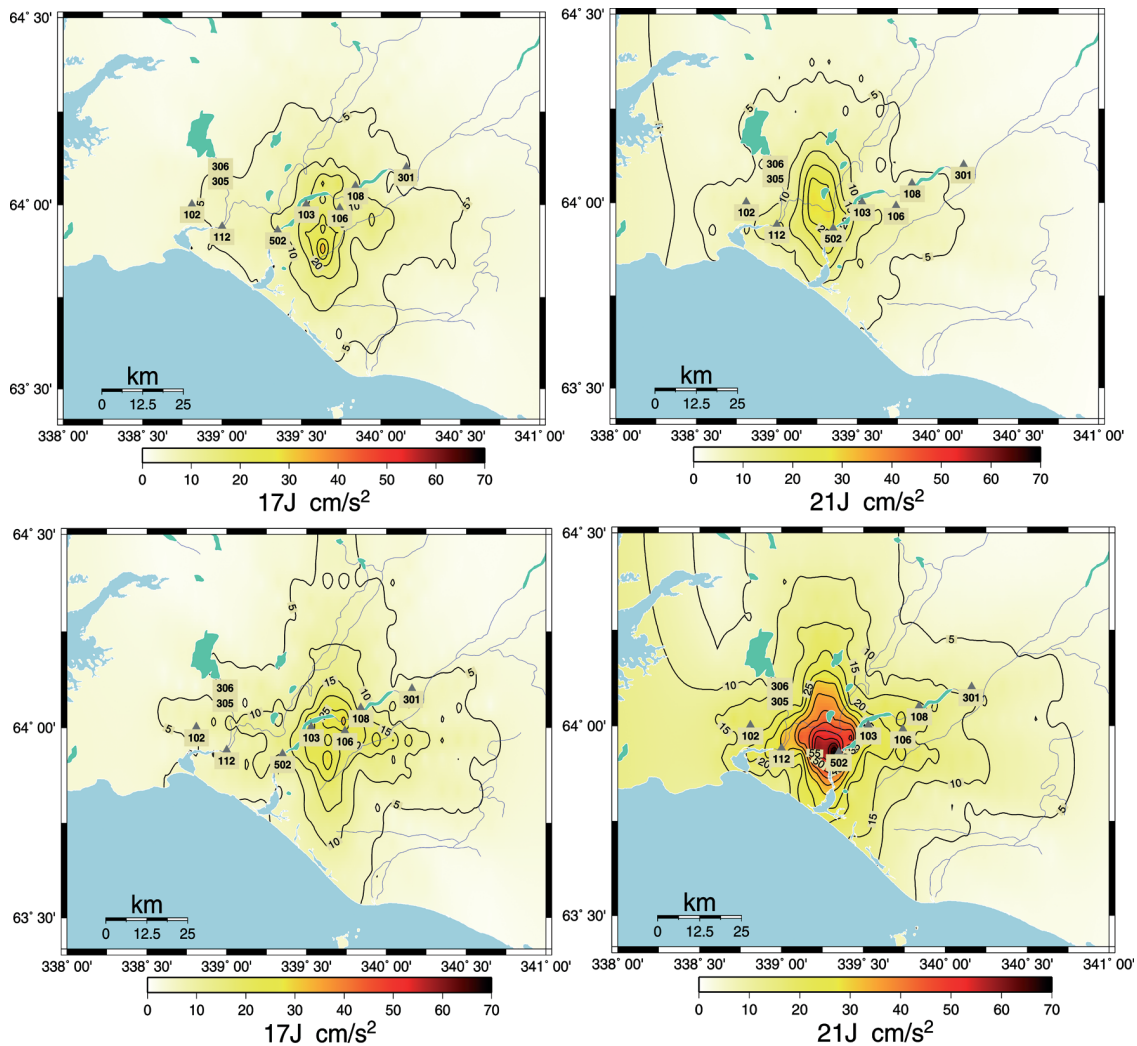
Fig. 6 - Contour maps of the resulting maximum horizontal spectral velocities for the 17 June event (left) and 21 June event (right). Top: the ground shaking scenario calculated using a uniform seismic moment distribution. Bottom: the ground shaking scenario computed using the seismic moment distribution obtained from the inversion of observed data. Stations are shown as triangles and denoted by a number.

moment distribution obtained from the inversion of strong motion data (Fig. 5) the results (Fig. 6, bottom) are rather different in terms of ground shaking level.

Since our distribution has two maxima of slip release in the upper part of the fault plane and near the Earth's surface, for the 21 June event, the values of accelerations and the region affected by a high level of ground shaking are considerably larger than in the case of a uniform slip distribution. On the other hand, a moment slip distribution concentrated more at depth and in the central part of the fault's surface, like that obtained for the 17 June event, shows a less dramatic influence on the values of accelerations with respect to a uniform slip distribution model. The comparison of the real data filtered at 1 Hz (Fig. 7), on the other hand, shows that for the 17 June
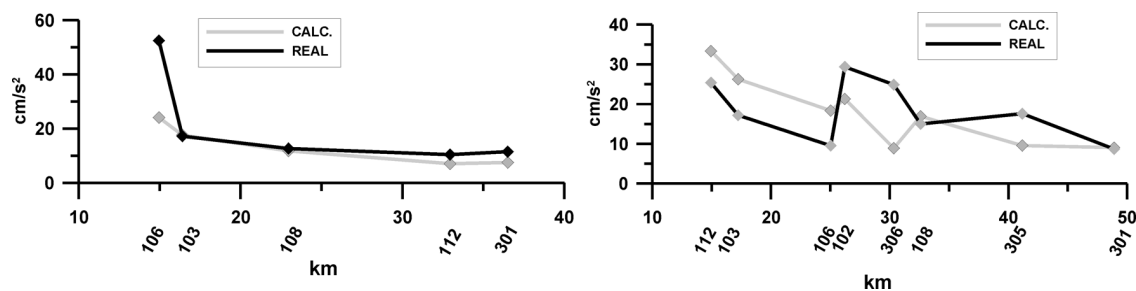
Fig. 7 - Comparison between the value of the maximum horizontal acceleration computed (fault slip distribution taken from Fig. 5 and, dashed, for a uniform distribution of moment) and the values, filtered at 1 Hz, recorded at the stations. Left: June 17 event. Right: June 21 event.

case a uniform moment distribution on the fault is an acceptable approximation (except at very short epicentral distances) to estimate the observed PGA distribution. For the 21 June event, though, at most of the stations, the agreement is acceptable only when using the inverted asperity model for the slip on the fault. Anyway, for distances less than 30 km the asperity model accelerations seem to be either slightly overestimated (15-25 km range) or slightly underestimated (25-30 km range). Since the stations used in the 17 June event are well reproduced also in the 21 June case, this might point to the fact that the stations with a worse fit might be affected by possible site effects that have not been taken into account.

4. Conclusion

The two simple examples of scenarios we have calculated, point out the importance of the slip distribution on the fault on the seismic hazard assessment in the surrounding region. In our kinematic approach, the well known parameters are the focal mechanism and the fault geometry, whose determination is also supported by the aftershock distributions and tectonic/geological settings. The effect of small variations of the strike, of the nucleation point and also of the used structural model have been tested by Costa *et al*. (2006b) for the Bovec 2004 event and do not appreciably affect the results. In general, applying a non-uniform seismic moment distribution we compute accelerations that are larger than those produced using a uniform moment distribution. However, the accelerations decrease more rapidly with the distance between the fault and the site, since large portions of the fault radiate small values of seismic moment. This fact is even more evident in the case of a single asperity. The importance of the location of asperities in depth is extremely important as proved by scenarios derived from the two Iceland 2000 earthquakes.

The inversion procedure to obtain the slip distribution on the fault surface and to evaluate the locations of the asperities should become a routine instrument for assessing the characteristic energy release on faults in active tectonic areas. In this way, the possible source-dependent variability of expected ground motion shaking could be easily estimated. From this point of view, predicting the locations of asperities in future earthquakes is a challenging topic of ongoing research.

REFERENCES:

Aoudia A.; 1998: *Active faulting and seismological studies for earthquake hazard assessment.* Ph.D. Thesis, University of Trieste, 152 pp.

Archuleta R.J. and Hartzell S.H.; 1981: *Effects of fault finiteness on near-source ground motion*. Bull. Seismol. Soc. Am., **71**, 939-957.

Carulli G.B., Nicolich R., Rebez A. and Slejko D.; 1990: *Seismotectonics of the Northwest External Dinarides*. Tectonophysics, **179**, 11– 25.

Costa G., Suhadolc P., Delise A., Moratto L., Furlanetto E. and Fitzko F.; 2006a: *Estimation of the site effects at some stations of the Friuli (NE Italy) accelerometric network (RAF).* In: Third International Symposium of the Effects of Surface Geology on Seismic Motion, Grenoble, France, 30 August – 1 September 2006, Paper number 89, LCPC, Paris, pp. 729-739.

Costa G., Delise A., Furlanetto E., Gergolet M., Moratto L., Sandron D. and Suhadolc P.; 2006b: *Bollettino della Rete Accelerometrica del Friuli- Venezia Giulia Anno 2005*. Dipartimento di Scienze della Terra, Università di Trieste, Relazione Interna, Marzo 2006.

Das S. and Kostrov B. V.; 1990: *Inversion for seismic slip rate and distribution with stabilizing constraints: application to the 1986 Andreanof Islands earthquake*. J. Geophys. Res., **95**, 6899-6913.

Das S. and Kostrov B. V.; 1994: *Diversity of solutions of the problem of earthquake faulting inversion. Application to SH waves for the great 1989 Macquarie Ridge earthquake*. Phys. Earth Planet. Inter., **85**, 293-318.

Das S. and Suhadolc P.; 1996: *On the inverse problem for earthquake rupture. The Haskell-type source model.* J. Geophys. Res., **101**, 5725-5738.

Fiztko F.; 2003: *Seismic hazard at the Alps-Dinarides junction-The 1511 earthquake*. PhD Thesis, University of Trieste, 203 pp.

Fiztko F., Suhadolc P. and Costa, G.; 2004: *Realistic strong round motion scenarios for seismic hazard assessment studies at the Alp-Dinarides Junction.* In: Chen Y.T., Panza G.F. and Wu Z.L. (eds), Earthquake Hazard, Risk, and Strong Ground Motion, Seismological Press. Beijing, pp. 361-377.

Florsch N., Fäh D., Suhadolc P. and Panza G.F.; 1991: *Complete synthetics seismograms for high frequency multimode SH waves.* In: Udias A. and Buforn E. (eds), El Escorial workshop proceedings, Pageoph, **136**, 529-560.

Herrero A. and Bernard P.; 1994: *A kinematic self-similar rupture process for earthquakes.* Boll. Seismol. Soc. Am., **84**, 1216-1228.

Kamae K., Irikura K. and Pitarka A.; 1998: *A technique for simulating strong ground motion using hybrid Green's function*. Bull. Seismol. Soc. Am., **88**, 357-367.

Panza G.F.; 1985: *Synthetic seismograms: the Rayleigh waves modal summation.* J. Geophys., **58**, 125-145.

Panza G.F. and Suhadolc P.; 1987: *Complete strong motion synthetics.* In: Computational techniques, vol. **4**, Seismic strong motion synthetics, Bolt B.A. (ed), Academic Press, pp. 153-204.

Panza G.F., Romanelli F. and Vaccari F.; 2001: *Seismic wave propagation in laterally heterogeneous anelastic media: theory and applications to the seismic zonation*. Advances in Geophysics, **43**, 1-95.

Press W. H., Flannery B. P., Teukolsky S. A. and Vetterling W. T.; 1986: *Numerical recipes: the art of scientific computing*. Cambridge University Press, New York.

Sandron D., Suhadolc P. and Costa G.; 2007: *Fault slip distribution of two June 2000 M_w 6.5 earthquakes in South Iceland estimated by strong motion inversion.* J. of Seismology, Submitted.

Saraò A., Das S. and Suhadolc P.; 1998: *Effect of non–uniform station coverage on the inversion for earthquake rupture*

history for a Haskell-type source model. J. of Seismology, **2**, 1-25.

Somerville P., Smith G., Nancy F., Graves R.W. and Abrahamson N.A.; 1997: *Modification of empirical strong ground motion attenuation relations to include the amplitude and duration effects of rupture directivity*. Seismological Research Letters, **68**, 199-222.

Somerville P. and Moriwaki Y.; 2003: *Seismic hazard and risk, assessment in engineering pratice*. In: International handbook of earthquake and engineering seismology, vol. **81B**, pp. 1065-1080.

Stefansson R., Gudmundsson B. and Halldorsson P.; 2003: *The South Iceland earthquakes 2000 a challenge for earthquake prediction research*. http://hraun.vedur.is/ja/prepared/SouthIcelandEarthq2000/SouthIceland Earthq2000_mar19_2003.html.

Swiss Seismological Service; 2006: http:// www.seismo.ethz.ch/

Wells D.L. and Coppersmith K.J.; 1994: *New empirical relationships among magnitude, rupture length, rupture width, rupture area, and surface displacement*. Bull. Seismol. Soc. Am., **84**, 974-1002.

Corresponding author: Denis Sandron
Dipartimento di Geofisica della Litosfera
Istituto Nazionale di Oceanografia e di Geofisica Sperimentale
Borgo Grotta Gigante 42c, 34010 Sgonico (Trieste), Italy
phone: +39 040 2140317; fax: +39 040 327307; e-mail: dsandron@ogs.trieste.it